Applied Catalysis A: General 408 (2011), 137-147

Palladium catalysts supported on N-functionalized hollow vapor-grown carbon nanofibers: The effect of the basic support and catalyst reduction temperature

S. Sahin [a], P. Mäki-Arvela [a], J.-P. Tessonnier [b], A. Villa [b], S. Reiche [b], S. Wrabetz [b], D.S.Su [b], R. Schlögl [b], T. Salmi [a], D.Yu. Murzin[a*]

[a] Process Chemistry Centre, Åbo Akademi University, Turku, FI-20500, Finland
[b]Fritz-Haber-Institut der Max-Planck-Gesellschaft, Faradagweg 4-6, 14195 Berlin, Germany

[*] Corresponding author: e-mail dmurzin@abo.fi,

Received: 26 July 2011; revised: 12 September 2011; accepted: 13 September 2011; available online: 19 September 2011

Abstract

The basic N-functionalized vapor-grown carbon nanofibers (N-VGCF) were synthesized by post-treating oxidized VGCFs in gaseous NH_3 at high temperature (ammonolysis) prior to Pd addition by sol immobilization. The catalysts were characterized by nitrogen adsorption, hydrogen temperature programmed desorption, adsorption microcalorimetry and by SEM and TEM. Catalytic activity was evaluated in a model reaction, synthesis of (*R*)-1-phenylethyl acetate starting from hydrogenation of acetophenone to racemic 1-phenylethanol over Pd supported on N-VGCFs, at 70 °C under atmospheric hydrogen pressure in toluene, followed by acylation over an immobilized lipase in the same reaction pot. The main parameters investigated in this work were the role of the basic N-VGCF supports as well as the reduction procedure of the supported Pd catalysts (Pd-N-VGCF). The results revealed that the catalytic activity of the Pd-N-VGCF catalysts was highly dependent on the reduction procedure. The highest desired product yield, 35%, was obtained over a Pd-N-VGCF catalyst when the support was treated at 400 °C with gaseous ammonia prior to Pd addition.

Keywords: Carbon nanofiber; Lipase; Hydrogenation; Pd

1. Introduction

The demand for single enantiomers of chiral intermediates raised in the pharmaceutical industry and thus considerable efforts are put on their production for the preparation of bulk drug substances [1, 2]. Aside from being useless, the biologically inactive enantiomers may display unwanted side effects. Therefore, regulatory authorities oblige the development of single enantiomers of chiral intermediates and their introduction to the market. This requires the development of processes to produce the enantiomer with the desired biological activity [3]. Kinetic resolution with enzymes is the most widely used method for separating the two enantiomers of a racemic mixture with the majority of kinetic resolution of racemates being performed with lipases [4a]. The main drawback of this method, however, is that the chemical yield is limited only to 50%. Some additional processes, such as separation, racemization and repeated resolution can be performed to increase the yield [5]. Furthermore, *in situ* racemization of the unwanted enantiomer over a racemization catalyst together with the enzyme [4, 6] is another way to increase the yield and thus to overcome this limitation.

The catalytic hydrogenation of acetophenone, which is one of the simplest molecules containing carbonyl and phenyl groups, is a complex reaction due to the presence of both these groups in one molecule [7]. The hydrogenation of acetophenone can produce racemic 1-phenylethanol through a carbonyl hydrogenation process. The consecutive reaction of dehydration to styrene with subsequent hydrogenation leads to ethyl benzene as a side product (Fig 1). Palladium based catalysts are widely used in the hydrogenation of acetophenone due to their high selectivity to hydrogenate only the carbonyl groups [8], as palladium properties could be modified to increase selectivity [9]. A sequential method, in which acetophenone was hydrogen

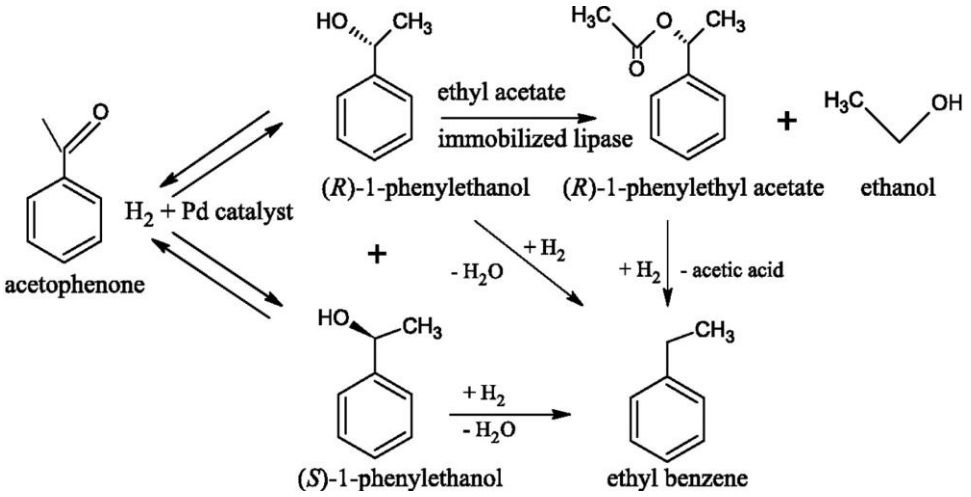

Figure 1. The reaction scheme for one-pot synthesis of *R*-1-phenylethyl acetate starting from acetophenone hydrogenation

ated over a heterogeneous Pd catalysts supported on either silica or alumina in the first step followed by the acylation with an immobilized enzyme in the second step was demonstrated [10]. The main product was ethyl benzene with a yield of 62% after 1600 min of reaction time for the preliminary experiments carried out over Pd/C and an immobilized enzyme catalyst. High ethyl benzene formation was due to the acid catalyzed dehydration by Pd/C of racemic 1-phenylethanol [11]. Since the results with Pd/C catalysts were not very good due to side reactions, other Pd catalysts such as basic Pd/MgO were tested in the one-pot synthesis of *(R)*-1-phenylethyl acetate [10]. Unfortunately, Pd/MgO exhibited the lowest initial rates among all tested catalysts, which was explained by the low surface area and low Pd dispersion. Nevertheless, only traces of ethyl benzene were formed over the basic Pd/MgO catalyst with the highest desired product selectivity at the same conversion levels [10]. A logical continuation of the previous work [10] consists therefore in the use of other basic supports. In this study, heterogeneous palladium catalysts supported on vapor-grown carbon nanofiber (VGCFs) were used for hydrogenation. The performance of the catalysts is significantly affected by their pretreatment conditions, as well as by the nature of the supports which play an important role in the catalytic activity and selectivity [10]. The VGCF supports were functionalized by treating them with gaseous ammonia at different temperatures prior to Pd addition. Depending on the treatment temperature, the basic character of the Pd catalysts supported on N-VGCF was changed.

VGCFs have become the focus of scientific and technological attention in the last two decades [13] due to their availability and relatively low price. They have a larger diameter than carbon nanotubes (CNTs) [14] and are produced by catalytic chemical vapour deposition (CCVD) method, based on the catalytic vapor phase decomposition of hydrocarbons such as methane, propane, acetylene, benzene, ethylene, etc. or carbon monoxide over metals (Fe, Ni, Au, Co) or metal alloys such as Ni-Cu, Fe-Ni [14]. Different morphologies and characteristics of VGCFs can be obtained depending on the feedstock, catalyst and operation conditions. The morphology of VGCFs is similar to that of multi-wall carbon nanotubes (MWCNT), and the major benefit of VGCFs over MWCNTs is that they are less expensive [15].

VGCFs have potential applications in batteries [19], in automotive industry [14] and in conductivity related applications. In addition, polymers filled with VGCFs are promising materials for biological applications such as the ones containing proteins and DNAs in the hollow core of fiber [20].

The aim of the present study was to report on (i) a preparation procedure and characterization of the N-functionalized Pd catalysts supported on vapor-grown carbon nanofibers (Pd-N-VGCF), ii) their application in the liquid phase selective hydrogenation of acetophenone into the corresponding alcohol under mild reaction conditions, i.e. at 70 ^{o}C and atmospheric pressure of hydrogen, and (iii) the effect of the catalyst reduction temperature on the one-pot synthesis of *(R)*-1-phenylethyl acetate starting from acetophenone.

2. Experimental

2.1. Synthesis of the N-functonalized supports

Vapor-grown carbon fibers (Pyrograf Products, USA, product PR24-PS) were used as starting material. A detailed characterization of this sample can be found in [21]. The vapor-grown carbon fibers (VGCFs) were first oxidized with concentrated nitric acid for 2 h at 100 °C, and then treated with gaseous NH_3 in tubular quartz reactor either at 200 ^{o}C, 400 ^{o}C or 600 °C for 4 h to create basic nitrogen-containing functional groups by ammonolysis [22].

2.2. Palladium deposition by sol immobilization

Palladium nanoparticles were deposited on the N-functionalized VGCFs (N-VGCFs) by immobilization of Pd^0 colloids [23]. Solid Na_2PdCl_4 (0.043 mmol) and 0.22 ml PVA solution (2%, w/w) (Pd/PVA 1:1, w/w) were added to 130 ml of H_2O. After 3 min, 0.860 ml of 0.1 M $NaBH_4$ solution was added to the yellow-brown solution under vigorous magnetic stirring. The brown Pd^0 sol was immediately formed. An UV–visible spectrum of the palladium sol was recorded for ensuring the complete reduction of Pd^{2+}. Within few minutes from their generation, the colloids (acidified at pH 2, by sulphuric acid) were immobilized by adding the support under vigorous stirring. The amount of support was calculated in order to obtain a final metal loading of 2 wt%. After 2 h the slurry was filtered and the catalyst washed thoroughly with distilled water. The prepared samples were finally dried at 100 °C overnight.

2.3. Characterization techniques

The catalysts were characterized by nitrogen adsorption method (Sorptometer 1900, Carlo Erba Instruments). The catalysts were out-gassed at 150 ^oC for 3 hours prior to the surface area measurements. The specific metal surface areas were calculated by using the BET equation. Temperature programmed reduction (TPR) of the fresh catalyst was carried out in 5 vol% H_2/Ar using a temperature ramp of 5 ^oC/min up to 400 ^oC using Micromeritics, Autochem 2910 apparatus. Temperature programmed desorption (TPD) was performed with a temperature ramp 5^oC/min under He flow. Prior to the desorption experiments, the catalysts were further reduced at either 100 ^oC or 200 ^oC, cooled down to room temperature and flushed with He for 30 min in order to remove any physisorbed hydrogen. The palladium (Pd) dispersion was determined by CO pulse chemisorption. Prior to measurements the catalysts were reduced either at 100 ^oC or 200 ^oC. Palladium stoichiometry was taken as 2 [22]. The acid-base titrations of the N-VGCF supports were performed as follows: 100 mg of sample was dispersed in 50 mL of 10^{-3} M KCl solution and stirred for overnight. Prior to measurements, the mixture was degassed under Ar for at least 1 h until the pH value was constant. The titration was carried out under Ar, using a 0.01 M HCl solution. The initial pH ($pH_{initial}$) values of the solution were recorded.

For adsorption microcalorimetry measurements A SETARAM MS70 Calvet calorimeter was combined with a custom-designed high vacuum and gas dosing apparatus, which has been described in detail in [24]. The dosing volume is 139 ml, and an absolute pressure transducer (MKS Baratron type 121) measures pressure variations of 0.003 mbar in this volume (provided the box temperature does not vary by more than ± 1.5 K), allowing (as a conservative estimate) to dose as low as 0.02 μmol into the sample cell. An all-metal cell was employed as described in [25], but without the basket-like insert. The degassing of the samples was conducted inside the calorimeter cell. After evacuation at 313 K to a pressure ≤ 10^{-8} mbar, the cell was closed. CO 3.7 (Westfalen) or CO_2 4.5 (Air Liquide) was introduced into the initially evacuated cell, and the pressure evolution and the heat signal were recorded for each dosing step. The adsorption isotherm was derived from the dosed amount and the equilibrium pressure (in comparison to an empty cell). The differential heats of adsorption were calculated by converting the signal area into a heat by using the calorimeter's calibration factor and then dividing the heat by the number of molecules adsorbed in this step. All data sets (consisting of one isotherm and the corresponding heats of adsorption) were obtained by treating a fresh sample.

The morphology and homogeneity of the samples were investigated with a Hitachi S-4800 scanning electron microscope (FE-SEM) equipped with SE and YAG-BSE detectors for imaging. The samples were loosely dispersed on conductive carbon tape. Images were first acquired with both SE and YAG-BSE detectors using an acceleration voltage of 15 kV in order to check the homogeneity of the samples, in particular the absence of any large metal aggregate. EDX spectra were also acquired at 15 kV primary electron energy. Quantification was done using the standard-less ZAF correction method in the Genesis software from EDAX. High magnification images were acquired using an acceleration voltage of 1.5 kV for better resolution of surface features. The microstructure of the reduced catalysts was investigated by high-resolution transmission electron microscopy (HRTEM), using a Philips CM200 FEG TEM operated at 200 kV. The samples were dispersed in chloroform and deposited on a holey carbon film supported on a Cu grid.

2.4. Experimental set-up

Typical experiments were performed at 70^oC in toluene (J.T. Baker, 99.5%) under atmospheric pressure of hydrogen (AGA, 99.999%) with a volumetric flow rate of 295 mL/min. To eliminate external mass-transfer limitations for substrates, the reaction media was stirred vigorously (500 rpm). The internal mass transfer was overcome by using small catalyst particles (< 100 μm). The liquid phase volume and the initial reactant concentration were 125 mL and 0.02 mol/L, respectively. Ethyl acetate (Sigma-Aldrich, >99.5%) with the concentration of 0.06 mol/l was used as an acyl donor. The catalytic hydrogenation of acetophenone (Acros, 99%) was carried out over 2% (w/w) Pd-N-VGCF (312.5 mg) and the formed *(R)*-1-phenyl ethanol was acylated in the same pot to *(R)*-1-phenyl ethyl acetate using an immobilized lipase (Novozym 435, 62.5 mg) (Fig 1). The experiments were performed with the following catalysts, which were all chemically reduced with $NaBH_4$ during synthesis (see 2.2): 1) fresh catalysts (catalysts without additional reduction

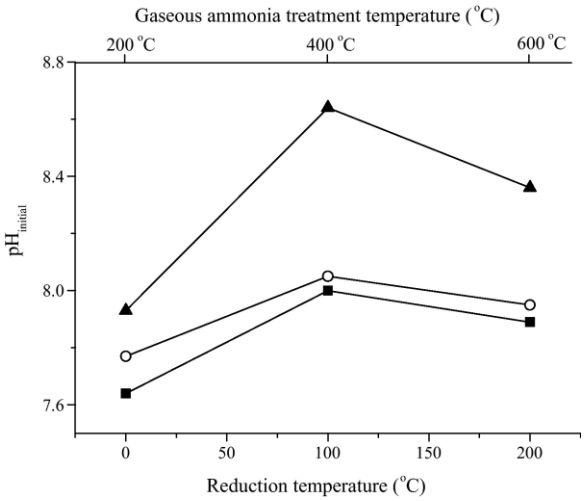

Figure 2. The $pH_{initial}$ as a function of reduction temperature (symbols; ▲: fresh catalysts, ■: supports reduced at 200 °C for 120 min under H_2 flow, ○: supports reduced at 100 °C for 30 min under H_2 flow).

prior to experiments), 2) catalysts reduced at 100 °C for 30 min, 3) catalysts reduced at 200 °C for 120 min.

2.5. Product analysis

The products were analyzed by a gas chromatograph equipped with a chiral column CP Chirasil Dex (Varian, USA) (250 μm × 0.250 μm × 25 m) and a flame ionization detector. The following temperature program was applied: 100 °C (1 min)–0.30 °C min^{-1} min–130°C–15 °C min^{-1} min–200 °C (10 min). The temperature of the injector and split ratio were 280 °C and 100:1, respectively. The products were identified using gas chromatography/mass spectrometry (GC-MS).

3. Results and discussions

3.1. Catalyst characterization

3.1.1. Acid-base titration

The solutions were always out-gassed by bubbling Ar for 1 h (until the pH was constant) before starting the measurement. The pH of the solutions progressively raised during the out-gassing because of the progressive desorption of CO_2 from the basic N-containing functional groups. All the samples analyzed gave relatively similar starting pH values ($pH_{initial}$). These $pH_{initial}$ values depend on the presence of O-containing groups created during the treatment with nitric acid and on the presence of basic N-groups formed by ammonolysis on the surface. The number and the nature of both the O- and N-groups are sensitive to the temperature of the NH_3 treatment [22, 26]. Acid-base titrations showed that during the additional reduction processes at 100 °C or 200 °C, many basic sites were lost, thus leading to lower pH values for the reduced catalysts than for the starting N-VGCFs supports (Fig 2). This might be due to the temperature-induced rearrangement of the N-containing groups, as already shown by Arrigo et al. [26] when heating similar supports in vacuum.

3.1.2.Temperature programmed reduction

TPR was performed for the fresh catalysts. Temperature reduction results for the fresh catalysts prepared by sol immobilization exhibited that higher reduction temperatures needed for the catalyst treated at 200°C with gaseous ammonia since the highest hydrogen uptake was at 310°C (Fig 3). The hydrogen uptake temperatures decreased with increasing gaseous ammonia treatment temperatures. A small negative peak with maximum at around 78°C can be attributed to decomposition of PVA, while a high temperature H_2 consumption peaks could have been associated with the reduction of Pd^{2+} ions to Pd^0 [27, 28]. However, since Pd catalysts prepared by sol immobilization were already (at least partially) reduced (Pd^0), the treatment is in fact removing PVA from the surface rather than reduction of Pd^{2+} ions formed because of slight oxidation of Pd^0 by contact with air back to Pd^0. The maximum temperature for hydrogen uptake for the catalysts treated with gaseous ammonia either at 200°C, 400°C or at 600°C prior to Pd addition was 310°C, 242°C and 225°C, respectively (Fig 3). This result indicated that when the catalyst was treated at higher temperature with gaseous ammonia, it was easier to remove PVA.

3.1.3. Adsorption microcalorimetry study

In order to understand the influence of catalyst reduction by hydrogen, adsorption studies using microcalorimetry were performed with the support N-VGCF treated with ammonia at 400°C (sample A), 2wt%Pd on the same support with Pd particles covered with a protective agent PVA and chemically reduced with $NaBH_4$ during the catalyst synthesis (sample B) as well as 2wt% Pd when PVA was removed by H_2 reduction at 100°C for 30 min (sample C). In the results below the calorimetric sign criterion, i.e. positive energetic quantity for an exothermic process, was adopted.

Fig. 4a displays CO_2 adsorption isotherms at 313 K on these samples. It clearly follows from Fig.4a that introduction of Pd to N-VGCF673K Pd leads to a lower amount of adsorption places for CO_2 at the same partial pressure. The bare N-VGCF673K provides adsorption capacity of 15.4μmol/g, while presence of metal diminished adsorption capacity to approximately 9 μmol/g. The identical amount of basic surface site for the Pd catalysts reflects the same Pd loading in samples B and C. The Pd- N- VGCF673K exhibits roughly 6.4 μmol/g or 38% less basic surface sites than the Pd free supported materials, proving that oxygen and basic nitrogen surface species created during ammonia

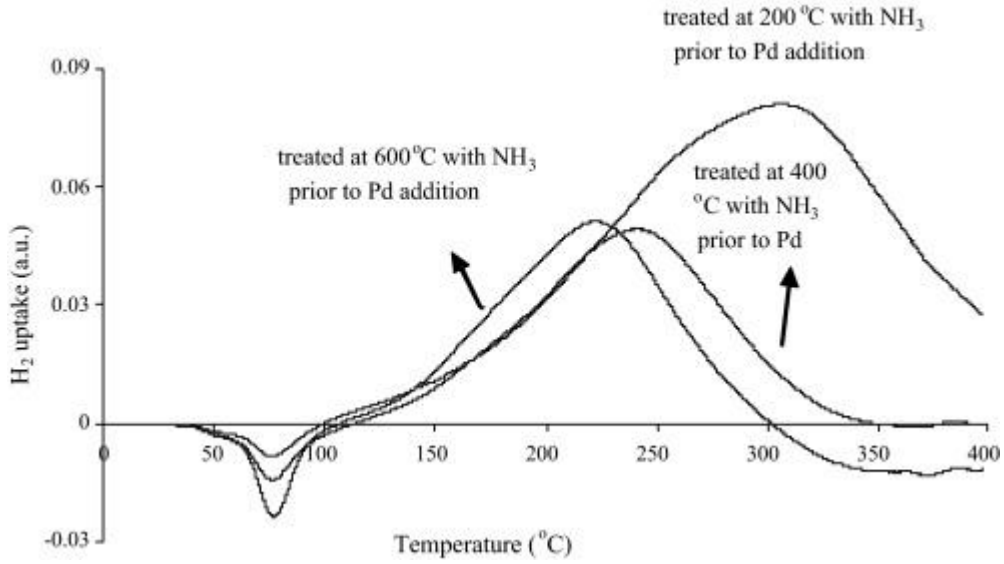

Figure 3. Temperature programmed reduction for the catalysts prepared by sol immobilization (SGI) and chemically reduced.

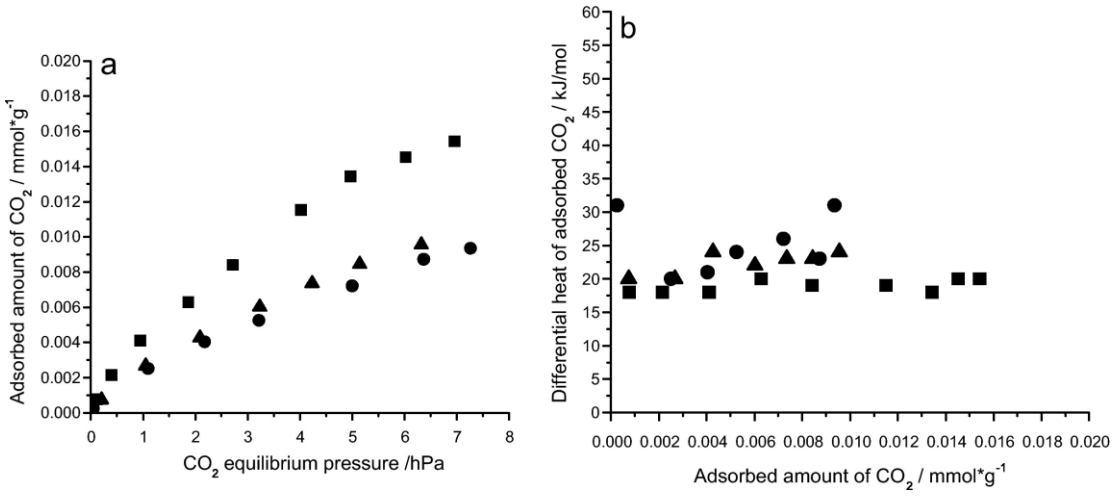

Figure 4. Adsorption of CO_2 at 313 K on samples C(circle), B (triangle) and A (square). (a) Isotherms and (b) differential heats as a function of coverage.

treatment represent the anchor sites for the metal nanoparticles**.**

The differential heats of adsorption as a function of adsorbed amount of CO_2 are reported in Fig. 4b. For all samples the heat profiles indicate an energetically homogeneous surface, although sample C exhibits few basic sites (< 0.3 µmol/g) with higher heat of adsorption. The final differential heat for samples containing Pd (B and C) was ca. 23 kJ/mol, while the bare support exhibits a final differential heat of 19 kJ/mol. It can be concluded that the basic surface properties are very weak, however, it seems that Pd doping gives rise to slightly stronger basic sites, which are still weak.

It is interesting to note that similar treated support material described in [26] shows differential heat of CO_2 of 50 kJ/mol, which could be at least partially associated with different storage time of these samples. The heat of CO_2 adsorption for the commercial VGCF is very low of ca. 30 kJ/mol. Furthermore, it is reported that depending on the amination temperature the N-VGCF surface provides energetically different basic sites which are heterogeneously distributed. It is obvious that the surface basic states are very sensitive to the preparation, oxidation and amination procedure. For CO_2 adsorption at 298 K on NaZSM-5 zeolite an initial differential heat of 53 kJ/mol and a final differential heat of 39 kJ/mol were observed indicating weak basic sites [29].

In all measurements CO_2 could be completely desorbed by evacuation at the adsorption temperature to a final pressure of ca. $3 \cdot 10^{-8}$ mbar. The resulting registered integral desorption heat ($q_{integral}$ = 30 mJ) was comparable to the sum of the heats for the individual adsorption steps ($q_{integral}$ = 33 mJ), indicating that CO_2 is reversibly adsorbed on all sample. The complete reversibility could be co

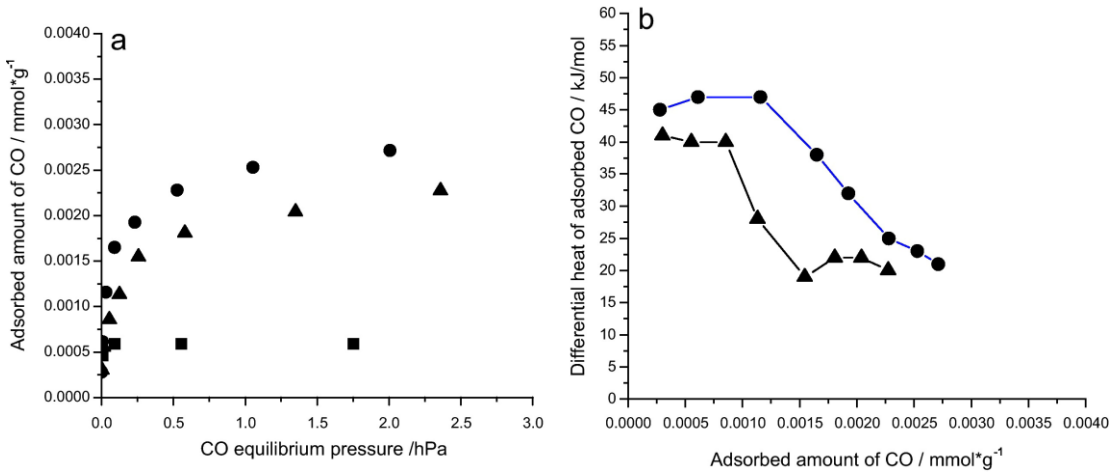

Figure 5. Adsorption of CO at 313 K on samples C(circle), B (triangle) and A (square). (a) Isotherm and (b) differential heats as a function of coverage.

Table 1. Catalyst characterization results

Entry	Catalyst	NH_3 treatment temperature (°C)	Metal dispersion (%)	Metal particle size (nm)	Metal specific surface area ($m^2 g^{-1}$)
1.1	Pd/N-VGCF	200[a]	13	8	32
1.2		200[b]	18	6	32
2.1	Pd/N-VGCF	400[a]	11	10	35
2.2		400[b]	19	6	35
3.1	Pd/N-VGCF	600[a]	9	12	29
3.2		600[b]	16	7	29

[a] Pd catalysts were pre-reduced at 100 °C for 30 min.
[b] Pd catalysts were pre-reduced at 200 °C for 120 min.

firmed by re-adsorption of CO_2 after desorption of CO_2 from the Pd containing samples (not shown).

The titration of the acidic properties of samples A, B and C using CO at 313K is reported in Fig. 5. The amount of adsorbed CO on sample C was negligible and consequently the corresponding heat signals were very small, therefore the differential heat could not be precise specified. This measurement is in agreement with the acid-base titrations and confirms that the acidic O-containing groups were fully replaced by basic N-containing groups by ammonolysis. The surface of the supports therefore consists of a mixture of weakly basic oxygen- and nitrogen-containing groups. In Fig.5a, the isotherms of the Pd containing samples could be attributed to the selective adsorption of CO on the Pd surface. As can bee seen from Figure 5a, reduction in H_2 results in higher amounts of accessible Pd sites, the difference being 0.44 µmol/g. These results are consistent with the TPR and demonstrated that H_2 led to a partial (~16%) removal of the PVA compared to chemical reduction, as well as to the reduction of any PdO formed by storage of the samples in air. The differential heat of CO adsorption as a function of the amount of adsorbed CO is shown in Fig. 5b. At low coverage, small heat plateau of around 47 kJ/mol for the sample C and 40 kJ/mol for the sample B indicate that both Pd catalysts exhibit a small amount of energetically uniform Pd sites; approximately 1.16 µmol/g for the former one and 0.86 µmol/g for the latter. At higher coverage the heat decreases rapidly indicating that in this range the monolayer is completed and multilayer adsorption proceeds. CO adsorption on ca. 2 wt%Pd supported on oxides (SiO_2, Al_2O_3, TiO_2, SiO_2/Al_2O_3) at 300 K after reduction at 573 K was reported in [30]. The initial differential heat of all samples was similar varying in the range of 93 to 136 kJ/mol. Large difference between this literature data and experimentally observed ones for the Pd/N-VGCF confirms the weak acidity of studied samples.

3.1.4. Surface area and metal dispersion

The total surface area determined from the BET equation (Table 1), ranges from 29 $m^2 g^{-1}$ to 35 $m^2 g^{-1}$. The low specific surface area of Pd-N-VGCF is due to the wall thickness of the N-VGCFs [31]. This observation is in agreement with a previous study showing a correlation between specific surface area, carbon nanotube diameter and number of walls [32].

The metal dispersions for the catalysts decreased with increasing gaseous ammonia treatment temperature when the catalysts were reduced at 100°C for 30 min under H_2 flow (Table 1, Entries **1.1**, **2.1**, **3.1**). Slightly higher metal dispersions were, however, achieved when these catalysts were reduced at 200°C for 120 min under H_2 flow (Table 1, Entries **1.2**, **2.2**, **3.2**) than when reduced at 100°C for 30 min under H_2 flow. This result can be explained by

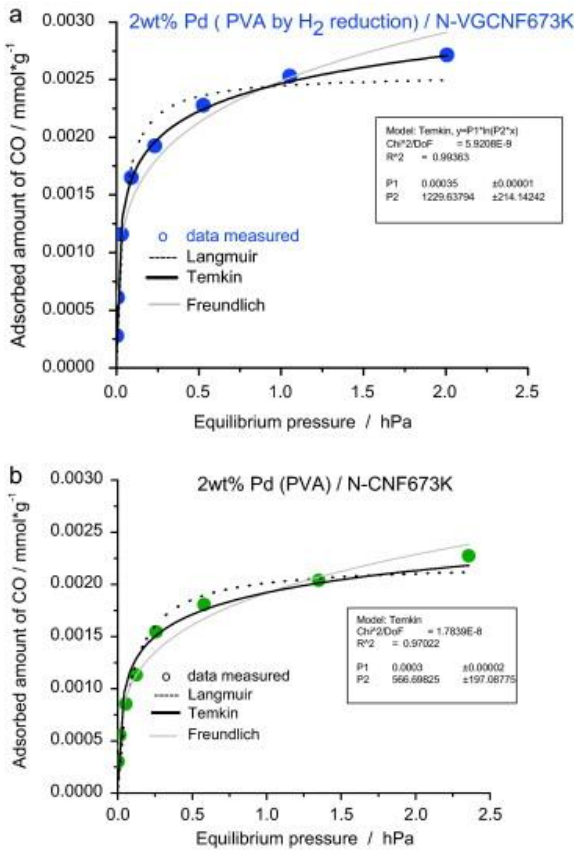

Figure 6. Adsorption isotherms of CO at 313 K on degassed a) 2wt% Pd (PVA removed by H_2 reduction)/N-VGCNF673K (sample C) and b) 2wt% Pd(PVA)/N-VGCNF673K (sample B)

the fact that PVA was not totally removed at 100 ^oC and probably still covered part of the Pd surface, while at 200^oC, all the PVA was removed. Furthermore, at 200^oC, no sintering took place.

A more detailed CO adsorption study was performed for samples A and B (see section 3.1.2). As could be seen from Figure 6 a simple Temkin (logarithmic) adsorption isotherm, which corresponds to energetically nonuniform surface, describes experimental data with reasonable accuracy, being in line with microcalorimetric study (Figure 5b).

For each sample, images were obtained with 15 kV in SE mode and in YAG-BSE mode since the electrons can go through the fibers as a result of the high accelerating voltage. Consequently, particles inside the VGCFs were observed. The YAG-BSE detector is very sensitive to heavy elements. Pd appears as very bright particles in the SE/BSE images, with diameters below 5 nm The metallic wires (bright lines) observed in some of the images actually correspond to encapsulated Fe, used as catalyst to grow the VGCFs by methane CCVD (Figures 7 and 8).

Most of the particles have a size of ca. 2 nm. The TEM images obtained from Entries **2.1** and **3.1** showed many small particles (Figures 9 and 10). Although not obvious in the metal dispersion measurements, some sintering/aggregation was observed for Entry **2.1** and even more Entry **3.1** such as melted like Pd particles.

3.1.5. Hydrogenation of acetophenone

In this work hydrogenation of acetophenone was carried out over 2% (w/w) Pd/N-VGCF catalysts differently pretreated. The previous studies [10, 11] conducted with palladium supported on active carbon (Pd-AC) catalyst in one-pot hydrogenation of acetophenone showed that ethyl benzene was formed as a major product due to the acidic support since typically Pd/AC catalysts exhibit acidic surface groups, such as carbonyl, carboxylic, phenolic hydroxyl, lactone and quinone groups. The influence of the acid-base properties of the support on the catalytic activity has been investigated by treating oxidized VGCFs with NH_3 at different temperatures in order to introduce various amounts of basic N-containing groups on the surface. The basic properties of the catalysts were increased by increasing the treatment temperature. The results shown in Table 2 demonstrated that the initial hydrogenation rates and conversions increased by increasing treatment temperature. No activity was observed with the supports alone (N-VGCF) which confirmed the need for the metal as an active hydrogenation site.

The effect of the pre-reduction procedure was also investigated. Preliminary experiments showed that if the hydrogenation catalysts were just reduced chemically during preparation without any pre-reduction with hydrogen, higher conversions were obtained after 480 min compared to pre-reduced samples. The hydrogenation catalysts, thus, were studied as such with chemical reduction or pre-reduced either at 200 ^oC for 120 min, 100 ^oC for 30 min under H_2 flow. The results explicitly indicated that the initial hydrogenation rates increased with decreasing pre-reduction temperature prior to the experiments.

3.1.6. Turnover frequency and initial rates

Turnover frequencies (TOF) were calculated (Table 2) taking into account metal dispersion. TOF values were in the range 0.4 10^{-3} s^{-1}-7 10^{-3} s^{-1} in line with the literature [33]. The highest TOF value was obtained over Entry **3.1** which was treated with gaseous ammonia at 600^oC and reduced at 100^oC for 30 min under H_2 flow prior to the experiment (Table 2). It was observed that the TOFs significantly increased with increasing ammonia treatment temperature (Fig. 11). Moreover, the TOFs increased with increasing average Pd particle size (Fig. 12). Recently similar cluster size effect, e.g. increase of TOF with an increase of ruthenium cluster size was observed in enantioselective hydrogenation of acetophenone [34].

The initial hydrogenation rates over the catalysts with supports treated with gaseous ammonia at 400^oC and 600^oC were 0.09 mmol/$min_{cat.}$ and 0.08 mmol/$min_{cat.}$, respectively. Higher initial hydrogenation rates were

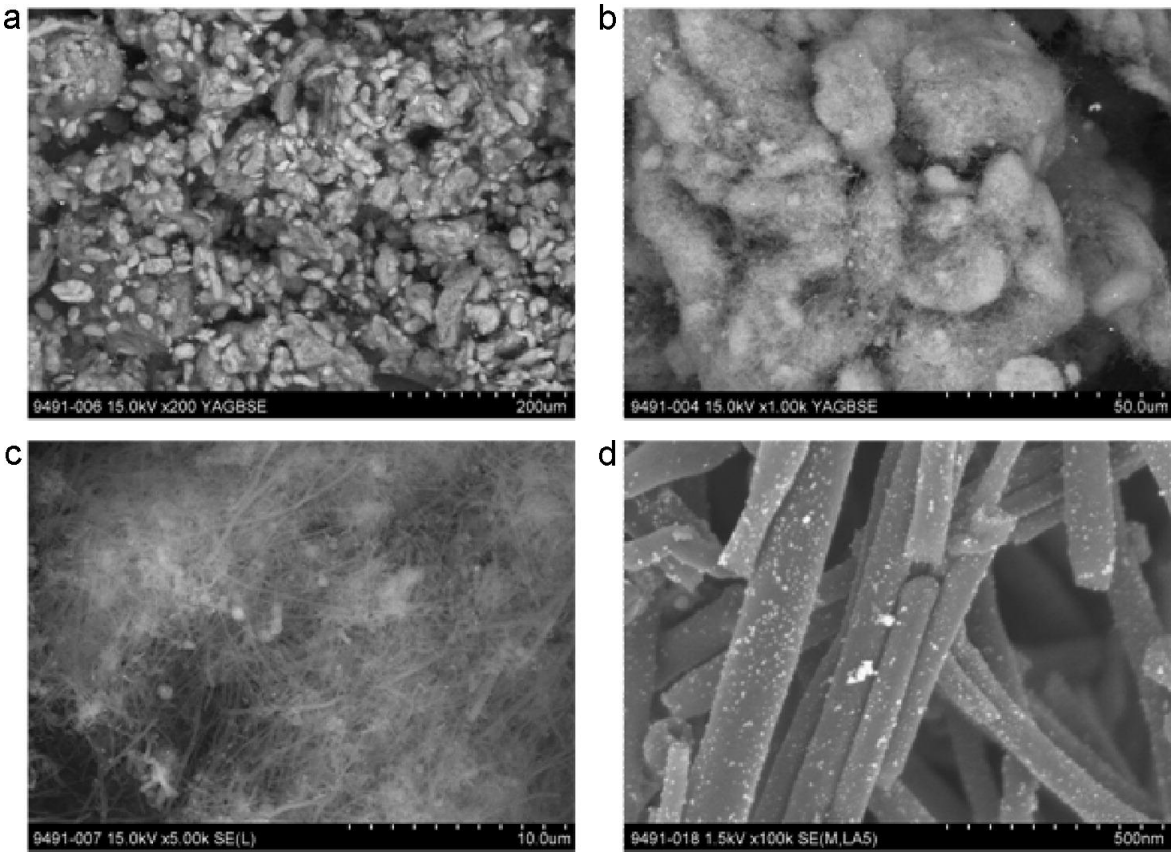

Figure 7. The SEM images of samples which were treated by gaseous ammonia at 400°C prior to Pd addition and reduced at 100°C for 30 min under H_2 prior to the reaction.

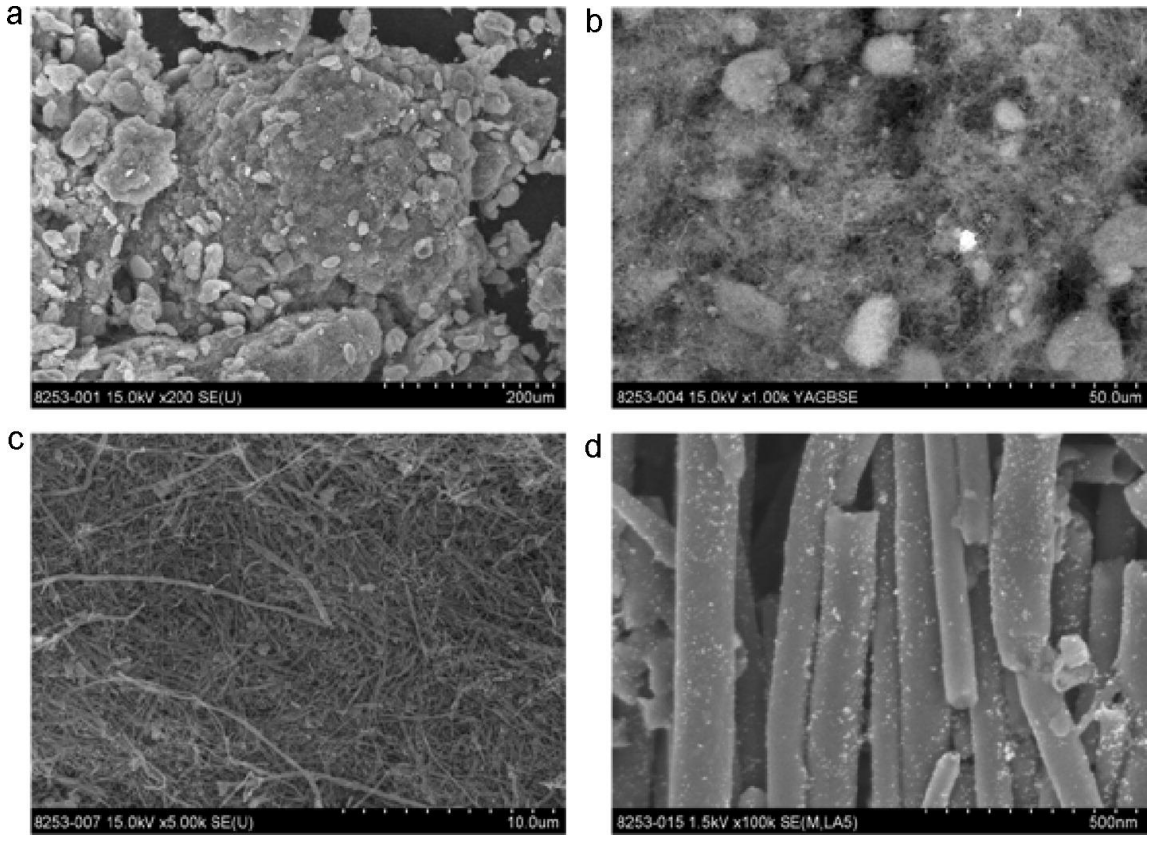

Figure 8. The SEM images of samples which were treated by gaseous ammonia at 400°C prior to Pd addition and chemically reduced

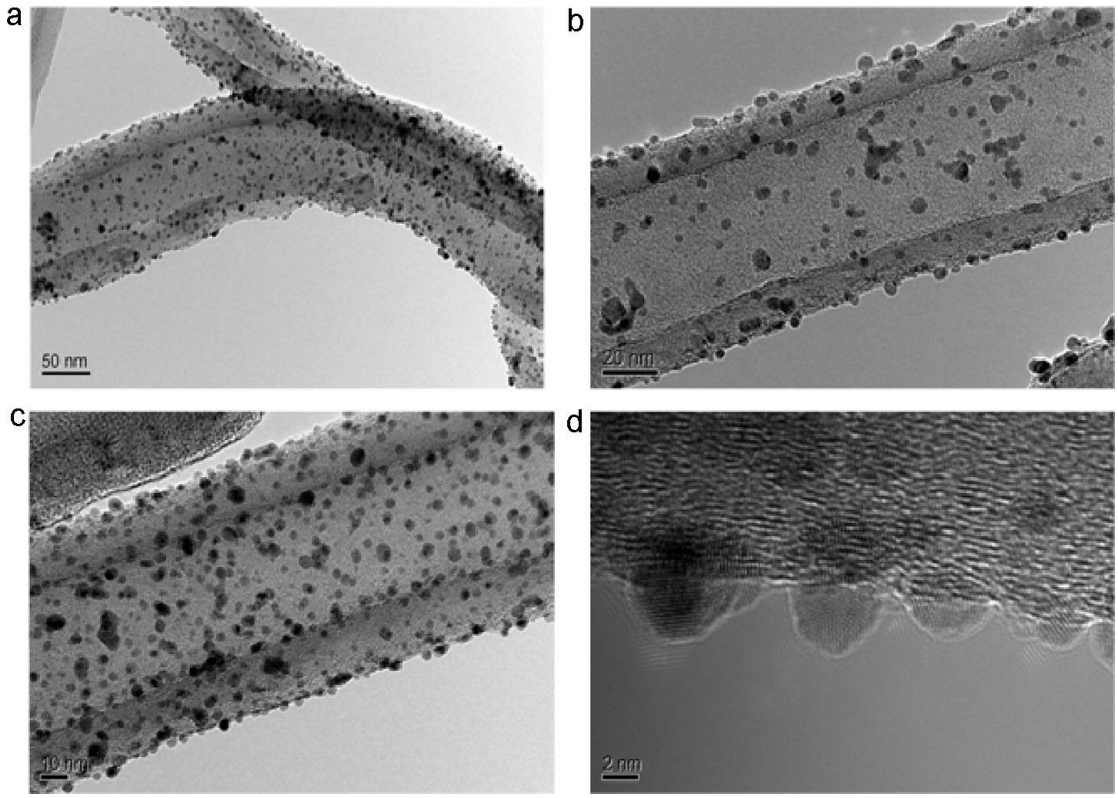

Figure 9. The HR-TEM images of samples which were treated by gaseous ammonia at 400ºC prior to Pd addition and reduced at 100ºC for 30 min under H_2 prior to the reaction.

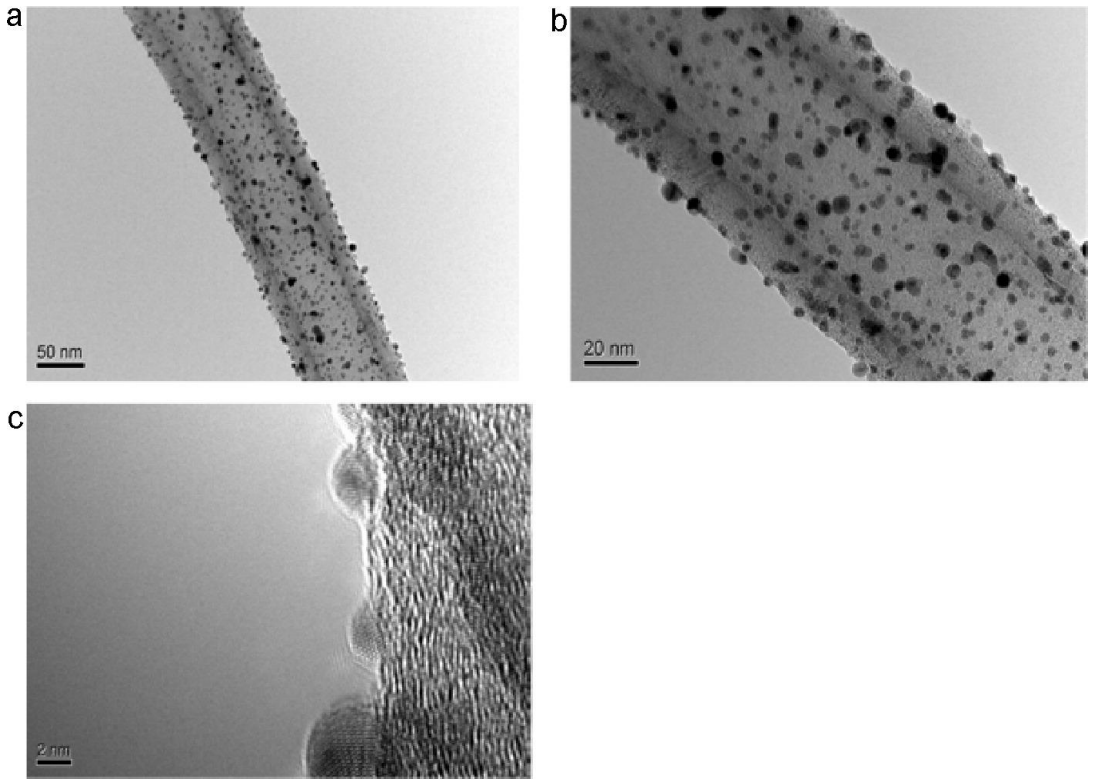

Figure 10. The HR-TEM images of samples which were treated by gaseous ammonia at 600ºC prior to Pd addition and reduced at 100ºC for 30 min under H_2 prior to the reaction.

Table 2. Kinetic results for the synthesis of *(R)*-1-phenylethyl acetate starting from acetophenone hydrogenation using Pd catalysts and immobilized lipase.

Entry	Catalyst	NH_3 treatment temperature (°C)	Initial hydrogenation rate (mmol/(min $g_{cat.}$))	TOF c × 10^3 (s^{-1})	Conversion after 300 min (%)	Conversion after 480 min (%)	Selectivity to (*R*)-PEAc (%)	EB selectivities (%)
1.0	Pd/N-VGCF[a]	200[a]	0.03	[i]	67	82 (97)[j]	19[d] (25)[e]	18[d] (20)[e]
1.1		200[b]	0.01	1	33	47 (78)[j]	38[d] (19)[f]	16[d] (15)[f]
1.2		200[c]	0.004	0.4	7	10 (30)[j]	17[d] (38)[g]	3[d] (5)[g]
2.0	Pd/N-VGCF[b]	400[a]	0.09	[i]	95	98 (99)[j]	15[d] (33)[e]	0[d] (8)[e]
2.1		400[b]	0.03	5	76	89 (98)[j]	26[d] (33)[e]	0[d] (10)[e]
2.2		400[c]	0.009	0.8	32	45 (75)[j]	32[d] (21)[h]	20[d] (15)[h]
3.0	Pd/N-VGCF[c]	600[a]	0.08	[i]	96	98 (98)[j]	6[d] (24)[e]	0[d] (7)[e]
3.1		600[b]	0.03	7	77	88 (98)[j]	22[d] (31)[e]	0[d] (11)[e]
3.2		600[c]	0.02	2	54	71 (94)[j]	27[d] (18)[e]	17[d] (15)[e]

[a] Pd catalysts without pre-reduction.
[b] Pd catalysts pre-reduced at 100 °C for 30 min.
[c] Pd catalysts pre-reduced at 200 °C for 120 min.
[d] Selectivities to (*R*)-1-phenylethyl acetate (*R*-PEAc) and ethyl benzene (EB) at 30% reactant conversion.
[e] Selectivities to (*R*)-PEAc and EB at 90% reactant conversion.
[f] Selectivities to *R*-PEAc and EB at 78% reactant conversion.
[g] Selectivities to *R*-PEAc and EB at 10% reactant conversion.
[h] Selectivities to *R*-PEAc and EB at 75% reactant conversion.
[i] CO pulse chemisorption was not performed for un-reduced Pd catalysts.
[j] The conversions in parenthesis were obtained after 1320 min reaction time.

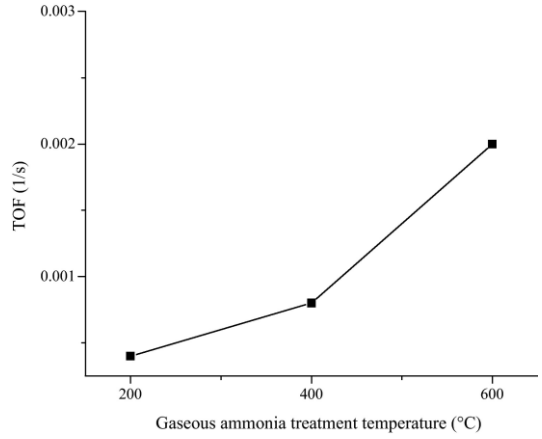

Figure 11. The TOFs as a function of ammonia treatment temperature for catalysts subsequently reduced at 200°C for 120 min under H_2 flow.

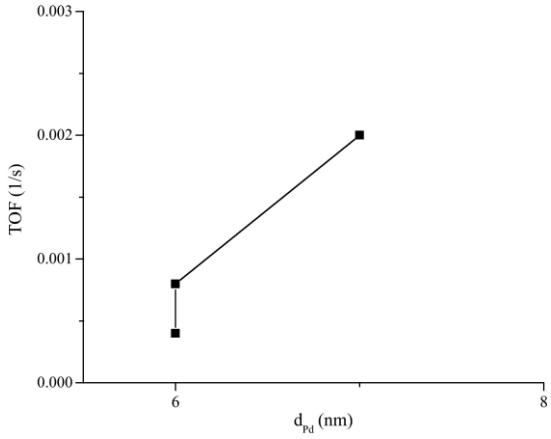

Figure 12. TOFs versus average Pd particle size for the catalysts subsequently reduced at 200°C for 120 min under H_2 flow.

achieved over the catalysts chemically reduced with subsequent reduction at 100 °C for 30 min under H_2 flow prior to the experiments than for the catalysts without such. The initial hydrogenation rates similarly to TOF increased with increasing gaseous ammonia treatment temperature.

3.1.7. Effect of ammonia treatment temperature on TOF and initial rates

Experiments with 2% (w/w) Pd/N-VGCF catalysts showed that the highest TOF was 7 10^{-3} s^{-1} over the catalyst treated with gaseous ammonia at 600 °C prior to Pd addition, followed by chemical reduction and further exposure to gaseous hydrogen for 30 min at 100 °C (Table 2, Entry **3.1**). The second highest TOF was 5 10^{-3} s^{-1} for Entry **2.1** (Table 2) when the support was treated at 400°C with gaseous ammonia and the catalyst was additionally reduced at 100°C for 30 min prior to the experiments.

The results indicated that TOF increases with increasing gaseous ammonia treatment temperature (Fig. 11). This trend showed also that the initial TOFs were higher when Pd catalysts with lower dispersion were applied.

3.1.8. Reaction rates and conversions after prolonged reaction time

The increasing ammonia treatment temperature increased the hydrogenation rates and acetophenone conversions after prolonged reaction times. Furthermore, the catalysts reduced only chemically exhibited higher rates and acetophenone conversions than the reduced ones (Table 2). Thus catalysts reduced at 200°C for 120 min exhibited lower conversions than the ones reduced at 100°C for 30 min under H_2 flow prior to the experiments.

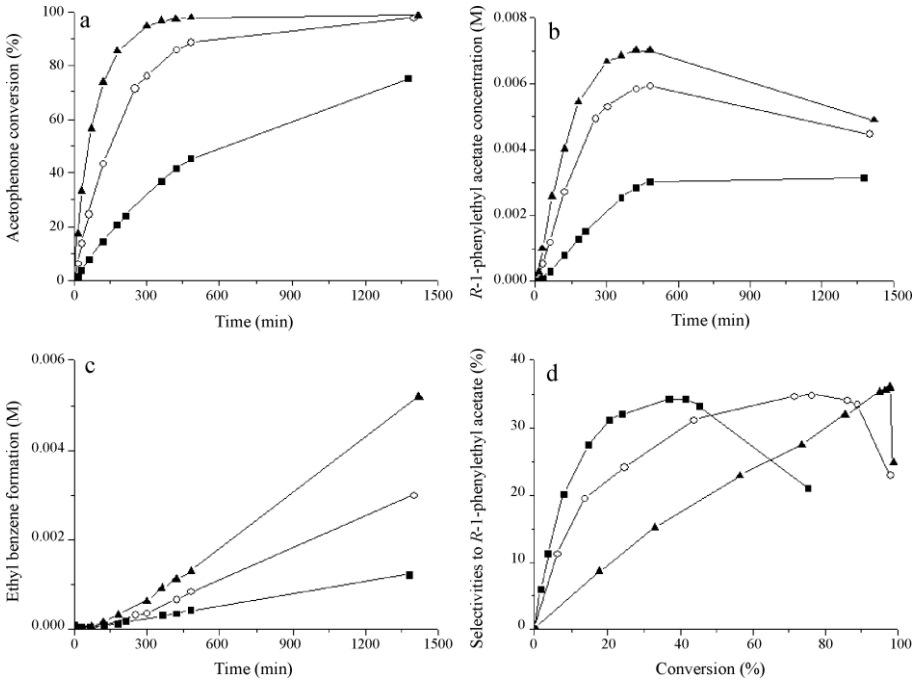

Figure 13. Kinetic results in one-pot synthesis of *(R)*-1-phenylethyl acetate a) acetophenone conversion, b) concentration of *(R)*-1-phenylethyl acetate, c) concentration of ethyl benzene and d) selectivities to *(R)*-1-phenylethyl acetate as a function of conversion. Catalysts were treated with gaseous ammonia at 200 °C prior to Pd addition (symbols; ▲: only chemical reductions, ○: additional reduction at 100°C for 30 min under H_2 flow, ■: additional reduction at 200 °C for 120 min under H_2 flow).

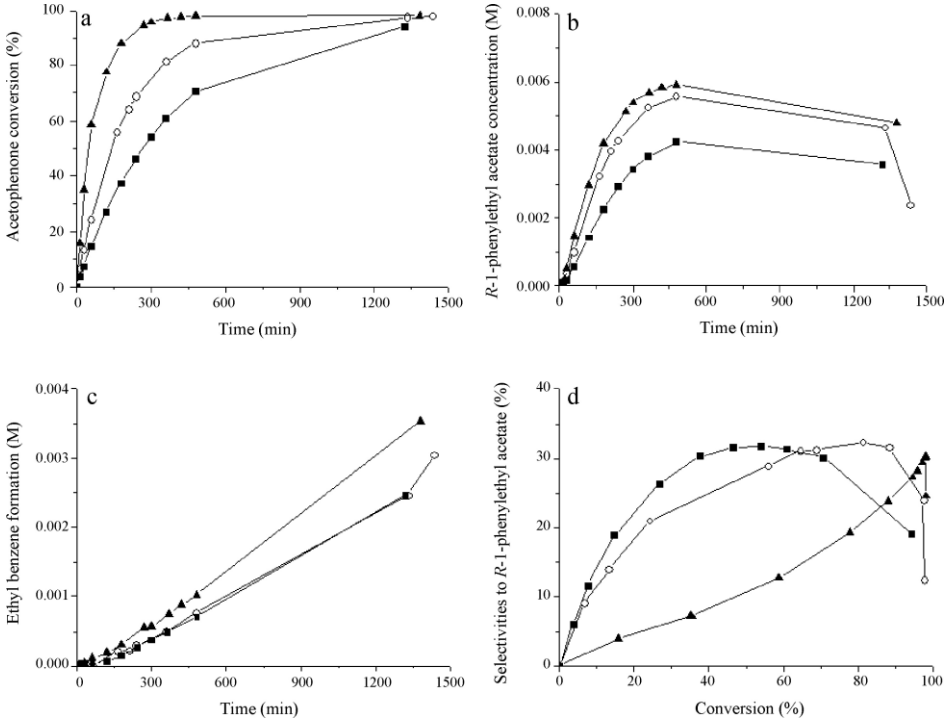

Figure 14. Kinetic results in one-pot synthesis of *(R)*-1-phenylethyl acetate a) acetophenone conversion, b) concentration of *(R)*-1-phenylethyl acetate, c) concentration of ethyl benzene and d) selectivities to *(R)*-1-phenylethyl acetate as a function of conversion. Catalysts were treated with gaseous ammonia at 400 °C prior to Pd addition (symbols; ▲: only chemical reductions, ○: additional reduction at 100°C for 30 min under H_2 flow, ■: additional reduction at 200 °C for 120 min under H_2 flow).

3.1.9. Effect of ammonia treatment temperature on conversions and product distributions in one-pot synthesis

Experimental results for one pot synthesis of *(R)*-1-phenylethyl acetate are given in Figures 13-15. The highest acetophenone conversion was 98% after 480 min with 36% selectivity to *(R)*-1-phenylethyl acetate (Table 2, Entry 2.0) in one-pot operation mode combining heterogeneous and enzymatic catalysts. In this entry the support was treated with gaseous ammonia at 400^{o}C prior to palladium addition and the catalyst was only reduced chemically (Fig 14a). Although, the catalyst prepared treated with gaseous ammonia at 600^{o}C prior to palladium addition and used without reduction by hydrogen (Table 2, Entry **3.0**) displayed the same acetophenone conversion, 98% after 480 min (Figure15a), the selectivity to *(R)*-1-phenylethyl acetate was 30% at this conversion (Fig 15d).

Ethylbenzene could be formed by dehydration of phenylethanol to styrene with subsequent hydrogenation to ethylbenzene (Figure 1) or debenzylation of the desired product (*R)*-1-phenylethyl acetate. Kinetic data (Figure 13-15) demonstrate that the concentration of latter product passes through a maximum, which is an indication of consecutive transformation of (*R)*-1-phenylethyl acetate. The basic sites in N-VGCF should in principle display low catalytic activity in dehydration reaction, which is catalyzed by acid sites. In order to check a hypothesis of dehydration catalysed by bases a separate experiment was performed with ZrO_2KCl catalyst (a basic catalyst with basic sites/CO_2 uptake 292 µmol/g and BET equal 57 m^2/g) resulting in the absence of any dehydration.

Partial removal of PVA during post catalyst synthesis reduction with hydrogen leads to higher initial selectivity to the desired product and much lower rates of ethylbenzene formation.

The maximum yield of *(R)*-1-phenylethyl acetate over Entry **2.0** was 35% at 98% conversion of acetophenone corresponding to 36% selectivity over 312.5 mg of Pd-catalyst in combination with 62.5 mg of immobilized lipase. The desired product yield was improved by using Pd-N-VGCF catalysts comparing to the yields obtained with Pd on active carbon as the maximal yield reported for the latter catalyst was 15% at 66% conversion of acetophenone [35]. In addition for one pot reaction with Pd on active carbon the major product was ethyl benzene due to the acidic character of the support.

4. Conclusions

The synthesis of *(R)*-1-phenylethyl acetate starting from acetophenone over Pd supported on N-functionalized vapor-grown carbon nanofiber (N-VGCF) in combination with an immobilized lipase at mild reaction conditions in toluene was successfully demonstrated in the present work. The effect of functionalization of vapor-grown carbon nanofibers by treatment with gaseous ammonia at various temperatures and the influence of different reduction procedures were in the focus of this study.

TOFs significantly increased with increasing ammonia treatment temperature and the highest TOF was obtained over the catalysts treated with gaseous ammonia at 600^{o}C, chemically reduced and subsequently treated at 100^{o}C for 30 min under H_2 flow prior to the experiment. Furthermore, TOFs increased with increasing average Pd particle size.

The highest acetophenone conversion was 98% after 480 min with corresponding selectivity to *(R)*-1-phenylethyl acetate of 36%. This is a significant improvement compared to utilization of palladium on active carbon catalysts, which result in significant ethylbenzene formation.

The effect of additional reduction with gaseous hydrogen after chemical reduction of Pd catalysts prepared by sol immobilization was significant leading, which could be in part explained by more complete removal of polyvinylalcohol (PVA), used during catalyst preparation.

Acknowledgements

This work is part of the activities at the Åbo Akademi Process Chemistry Centre within the Finnish Centre of Excellence Programme (2000-2011) by the Academy of Finland.

References

[1] R.N. Patel Enzyme Microb Tech 31 (2002) 804-826.
[2] M. Habulin, Z. Knez, J. Mol. Catal. B: Enzyme 58 (2009) 24-28.
[3] A. Overmeyer, S. Schrader-Lippelt, V. Kasche, G. Brunner, Biotechnol. Lett. 21 (1999) 65-69.
[4] a) L. K. Thalén, D. Zhao, J.-B. Sortais, J. Paetzold, C. Hoben, J-E. Bäckvall, Chem. Eur. J. 15 (2009) 3403–3410; b) A-B. L. Fransson, Y. Xu, K. Leijondahl, J-E. Bäckvall, J. Org. Chem. 71 (2006) 6309-6316.
[5] M-J. Kim, Y. Ahn, J. Park, Current Opinion in Biotechnology 13 (2002) 578–587.
[6] J. H. Koh, H. M. Jeong, J. Park, Tetrahedron Lett. 39 (1998) 5545-5548.
[7] C-S. Chen, H-W. Chen, Appl. Catal. A: General 260 (2004) 207-213.
[8] A. Drelinkiewicza, A. Waksmundzka, W. Makoski, J.W. Sobczak, A. Krol, A. Zieba, Catal. Lett. 94 (2004) 143-156.
[9] M. Lenarda, M. Casagrande, E. Moretti, L. Storaro, R.Frattini, S. Polizzi, Catal. Lett. 114 (2007) 79-84.
[10] P. Mäki-Arvela, S. Sahin, N. Kumar, J.-P. Mikkola, K. Eränen, T. Salmi, D. Yu. Murzin, Catal. Today 140 (2009) 70-73.

[11] P. Mäki-Arvela, S. Sahin, N. Kumar, J.-P. Mikkola, K. Eränen, T. Salmi, D. Yu. Murzin, React. Kinet. Catal. Lett. 94 (2008) 281-288.
[12] B. M. Reddy, K. N. Rao, G. K. Reddy, Catal. Lett. 131 (2009) 328-336.
[13] T. Ozkan, M. Naraghi, I. Chasiotis, Carbon 48 (2010) 239-244.
[14] M. H. Al-Saleh, U. Sundararaj, Carbon 47 (2009) 2-22.
[15] H. Miyagawa, M. Misra, A.K. Mohanty, J Nanosci Nanotechnol 5 (2005) 1593-1615.
[16] S. Iijima, T. Ichihashi, Nature 363 (1993) 603-605.
[17] D. S. Bethune, C.H. Kiang, M. S. de Vries, G. Gorman, R. Savoy, J. Vasquez, R. Beyers: Nature 363 (1993) 605-607.
[18] S. Iijima, Nature 354 (1991) 56-58.
[19] M. Endo, Y. A. Kim, T. Hayashi, K. Nishimura, T. Matusita, K. Miyashita, Carbon 39 (2001) 1287-1297.
[20] B. S. Shim, J. Starkovich, N. Kotov, Compos. Sci. Technol. 66 (2006) 1174-1181.
[21] J.P.Tessonnier, D. Rosenthal, T.W. Hansen, C. Hess, M.E. Schuster, R. Blume, F. Girgsdies, N. Pfander, O. Timpe, D.S.Su, R. Schlogl, Carbon 47 (2009) 1779-1798.
[22] R. Arrigo, M. Hävecker, R. Schlögl, D.S. Su, Chem.Commun. 40 (2008) 4891-4893.
[23] D. Wang, A. Villa, F. Porta, D.Su, L. Prati *Chemm.Comm.* (2006), 1956-1958
[24] L.C. Josefowicz, H.G. Karge, E.N. Coker, J. Phys. Chem. 98 (1994) 8053-8060.
[25] E.N. Coker, H.G. Karge, Rev. Sci. Instrum. 68 (1997) 4521-4524.
[26] R. Arrigo, M. Hävecker, S. Wrabetz, R. Blume, M. Lerch, J. McGregor, E. P. J. Parrott, J. A. Zeitler, L. F. Gladden, A. Knop-Gericke, R. Schlögl, D. S. Su, JACS,.132 (2010) 9616-9630
[27] C. Amorim, G. Yuan, P. M. Patterson, M. A. Keane, J. Catal. 234 (2005) 268-281.
[28] A. Pintar, J. Batista, J. Hazard. Mater. 149 (2007) 387-398.
[29] A. Auroux, J.C. Vedrine, In "Catalysis by Acids and Bases", p.311, Elsevier, Amsterdam, 1985
[30] N. Cardona -Martinez and J.A. Dumesic, Adv. Catal., 38 (1992) 149-244.
[31] P. Serp, M. Corrias, P. Kalck, Appl. Catal. A. 253(2003) 337-58.
[32] A. Peigney, C. Laurent, E. Flahaut, R. R. Bacsa, A. Rousset, Carbon 39 (2001) 507-14.
[33] F. Jutz, J. M. Andanson, A. Baiker, J. Catal. 268 (2009) 356-366.
[34] L. Ye, H. Lin, H. Zhou, Y. Yuan, J. Phys. Chem. C, 114 (2010) 19752–19760
[35] S. Sahin, P. Mäki-Arvela, J.-P. Tessonnier, A. Villa, L. Shao, D. Sheng Su, R. Schlögl, T. Salmi, D. Yu. Murzin, Stud. Surf. Sci. Catal. 175 (2010) 283-287.